sustainability

Article

Land Use/Land Cover Changes in a Mediterranean Summer Tourism Destination in Turkey

Ismail Cinar [1], Zeynep R. Ardahanlıoğlu [1] and Süleyman Toy [2,*]

1 Department of Landscape and Ornamental Plants, Mugla Sitki Kocman University, 48000 Fethiye, Turkey; icinar@mu.edu.tr (I.C.); zeyneprb@mu.edu.tr (Z.R.A.)
2 City and Regional Planning Department, Architecture and Design Faculty, Atatürk University, 25240 Erzurum, Turkey
* Correspondence: stoy58@gmail.com or suleyman.toy@atauni.edu.tr; Tel.: +90-442-231-6110

Abstract: Tourism contributes to national and local economies especially in the Mediterranean and Aegean coasts of Turkey including the study area, Fethiye-Göcek, Muğla in southwest Turkey. The study evaluates land use/land cover (LULC) changes driven by tourism development as a case considering the past (1995–2020) and future environmental impacts on the area. High-resolution remote sensing and some socio-economic data were employed to monitor the situation and causes of LULC changes using Normalised Difference Vegetation Index (NDVI) and Land Surface Temperature (LST). The results show a decrease in the size of water surface, forest and maquis lands due to tourism development together with an increase in urban fabrics and bare lands due to urbanisation and forest fires. A significant positive correlation was detected between the urbanisation rate, population size and built-up area as well as air temperature and LST. Rapid and unplanned tourism development boosted investments for infrastructure and facilities and thus increased the demands for lands. Such lands were mostly gained by filling the sea or transforming agricultural and greenhouse areas, forest and maquis-covered lands. The unplanned development of tourism and urban areas caused serious hazards to the natural and cultural areas which threaten the sustainability of tourism. Planning suggestions are proposed to decision makers like coordination works for sustainable and responsible tourism development.

Keywords: tourism development; land use/land cover change; land surface temperature; Fethiye-Göcek

check for updates

Citation: Cinar, I.; Ardahanlıoğlu, Z.R.; Toy, S. Land Use/Land Cover Changes in a Mediterranean Summer Tourism Destination in Turkey. *Sustainability* **2024**, *16*, 1480. https://doi.org/10.3390/su16041480

Academic Editor: Harry Coccossis

Received: 16 January 2024
Revised: 25 January 2024
Accepted: 31 January 2024
Published: 9 February 2024

1. Introduction

Land use/land cover (LULC) changes are counted among the most important human-induced external forcings to Earth's climate system as well as greenhouse gas emissions (GHG) from fossil fuel combustion in industrial and urbanisation processes [1].

LULC changes, which result mainly from human population increase due to natural or compulsory processes like migration at a specific point, refer to a conversion or transformation of rural/natural lands covered generally by vegetation into urban areas, agricultural lands or other functions where human activities are dominant [2]. Such changes result in albedo differences and decayed atmospheric features due to emitted greenhouse gases and aerosols, and radiative forcing (i.e., local, regional or global warming; [1,3–5]). The changes in LULC are in fact the result of the ever-increasing demand for space as a result of a nation's adopted socio-economic policies and systems. The changes in LULC types can be affected by economic development preferences like those involving the manufacturing or construction sector, even land rent depending on the service industry which needs and triggers new lands to build facilities and land valuation [6–10]. As a developing country, Turkey has experienced all of the aforementioned examples of changes in LULC in its modern history since the 1950s when a great rural migration to industrialising cities occurred, where unprecedented urban sprawls were created in an unplanned and illegal manner, then from the 1980s onwards urban sprawls on farmlands and land transformations leading to increased urban density [11] continued based on land rent due to economic growth and population increases in metropoles as in other countries of the world (e.g., China; [12–16]). Causes, sizes, results and management of the changes in LULC have long been on the agendas of policymakers and scientific literature which focuses on the spatial and temporal aspects as well as the driving forces at specific scales [16–19].

The tourism industry has taken place among the most important socio-economic development opportunities in Turkey since especially the mid-1980s and sectoral indicators (like arrivals, overnights etc.) have increased with only a few interruptions (like the political crises, terror attacks and 2020/21 COVID-19 pandemic). For instance, the number of travellers and tourism revenue of the country have increased every year over the last three decades. Turkey shelters three of the 100 most popular tourism destinations in the world [20]; i.e., Istanbul, Antalya and Muğla, which have cultural heritages and sea, sand and sun tourism potential from the Aegean and the Mediterranean Sea and are ranked the 9th, 12th and 81st by hosting 14.7, 13.3 and 2.92 million visitors in 2019, respectively.

Tourism is among the largest and fastest growing economic sectors in the world, including in Europe and Turkey, which generates serious employment rates (one in 10 jobs around the world) and contributes to local, regional and national socio-economic development [21], community welfare and conservation of natural and cultural assets [22]. Many countries, including Turkey, which give priority to tourism in their long-run development pathways are in fierce competition to benefit from larger shares of tourist revenue and employment [23,24]. The tourism industry is also associated with some negative impacts on nature and the climate, like causing changes in LULC and increasing GHG emissions besides being vulnerable to climate-related risks [22,25]. As a labour-intensive sector, tourism involves numerous human activities in its value chain and requires spatial organisations for the development of accommodation facilities, entertainment areas (such as infrastructures like pools etc.), transport infrastructures, food and beverages facilities etc. Therefore, the sector causes, drives and triggers LULC changes since it also creates attractive points for financial investments, land valuation and impacts on other subsectors in the value chain of the sector [26]. Efforts to meet strong demands for land due to the rapid tourism development which has also been prioritised mainly by omitting the sustainability of natural and cultural resources due to competition is beginning to cause irreversible outcomes especially in the forest and coastal areas [27,28] and farmlands.

Coastal regions of Turkey began to be occupied by the functions involving tourism-related activities from the early 1970s [29]. Aggressive investment for both infrastructure by the government and facilities by private sector tourism development has been causing LULC changes together with numerous impacts on natural and cultural heritages. Muğla province, which is among such areas located in the southwest part of Turkey, ranks as the 3rd largest destination in the country to host visitors especially in summer for its unique nature, sea (Mediterranean and Aegean) and cultural heritage. The study area, Fethiye district is located on the border of Muğla province and is also a world-famous summer tourism destination. With the development of the tourism industry in the area, a dramatic change has been experienced in LULC in the study area which also covers Fethiye-Göcek Special Environmental Protection Area (SEPA) where critical protection priorities are offered for special conservation needs.

Even though the impacts of coastal tourism-related human activities on LULC changes have long been investigated to show the need for planned and sustainable tourism development in the most demanded parts of the Mediterranean region in Turkey like Antalya [29], Datça and Bodrum (Muğla) [30,31], there is still a need in the literature to follow these impacts periodically in different parts of the region where tourism and related human activities densify year by year. Therefore, the aim of the present study is to monitor the spatial and temporal LULC changes in the Fethiye district between 1995 and 2020 associated with tourism development. The study follows the changes in LULC through NDVI and land surface temperature (LST) and evaluates the impacts of the changes driven by tourism activities on the environment to offer suggestions for local governments and decision makers to manage lands and sustainable tourism. The study can also contribute to the literature on the changes in LULC driven by tourism in the sample of the 3rd largest tourist destination in Turkey as a case study.

2. Materials and Methods

2.1. Study Area

The Mediterranean region of Tukey has faced abrupt and dense LULC changes in recent times where natural ecosystems including coastal areas and the sea were largely transformed into built-up areas for various aims, mainly tourism-dependent development [31]. The study area was selected as Fethiye–Göcek SEPA in Muğla province in the farthest southwest area of Turkey (36°37′ N; 29°07′ E). The area is a worldwide famous summer tourism destination. It is located on the ancient city of Lycian with a recorded history starting in the 5th century BC. The area is in the cross-section of the Mediterranean and Aegean geographic regions. Very hot, dry and long summer and cool and rainy winter conditions are prevalent in the area with the average climatic values given in Table 1. The prevailing wind direction is west during the daytime and east at night time. The study area is located in an isolated basin with mountains that run perpendicular to the coast with an open valley to the sea winds (Figure 1).

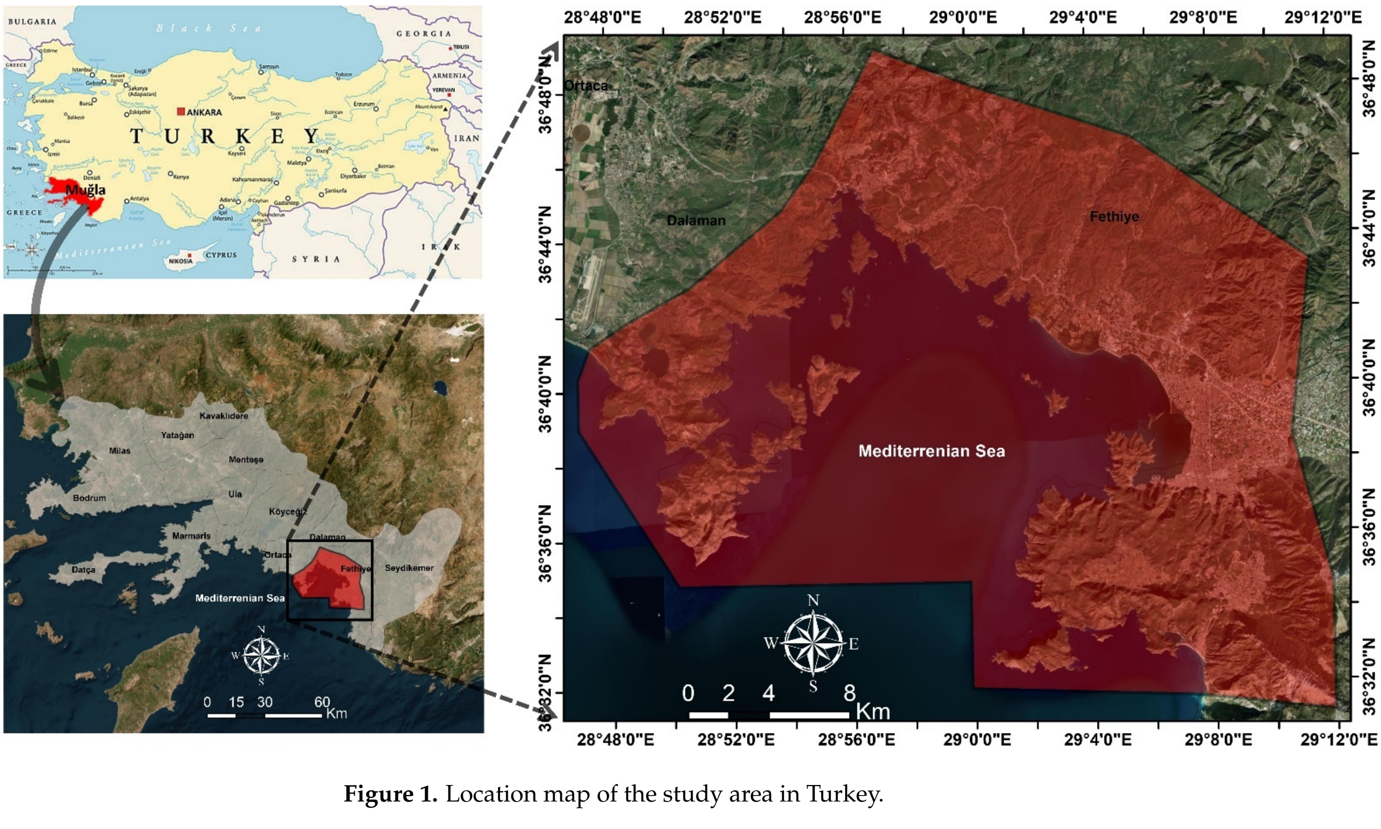

Figure 1. Location map of the study area in Turkey.

The area attracts a considerable number of tourists every year. Muğla province totally accounts for above 5% of the country's total tourist arrivals (domestic and international) while the Fethiye district also attracts nearly 10% of the total tourist numbers in Muğla on average between 2015 and 2020 (Table 2).

Table 1. Average values of meteorological parameters [32].

MUGLA Measurement Period (1928–2022)	January	February	March	April	May	June	July	August	September	October	November	December	Annual
Mean temperature (°C)	5.3	6.1	8.5	12.8	17.8	22.8	26.4	26.3	21.9	16.2	10.8	7.0	15.2
Mean maximum temperature (°C)	9.8	11.0	14.1	18.9	24.3	29.6	33.4	33.6	29.3	23.1	16.7	11.5	21.3
Mean minimum temperature (°C)	1.6	1.9	3.5	7.0	11.4	16.1	19.7	19.6	15.3	10.3	5.9	3.2	9.6
Mean sun shine duration (hour)	3.5	4.4	5.7	7.3	8.7	10.5	11.4	10.9	9.5	6.8	4.7	3.3	7.2
Mean number of rainy days	14.95	12.32	10.47	8.61	7.37	3.72	1.52	1.41	2.62	6.32	9.67	14.53	93.5
Monthly total rainfall (mm)	245.7	178.3	122.4	63.7	49.9	24.6	11.7	14.6	23.1	72.8	135.6	265.0	1207.4
Extreme maximum temperature (°C)	20.9	25.5	28.8	31.6	39.4	40.8	42.1	41.2	39.2	36.8	29.0	23.8	42.1
Extreme minimum temperature (°C)	−12.6	−9.9	−8.5	−3.6	1.0	6.7	10.5	9.0	5.6	0.1	−7.0	−9.0	−12.6

Table 2. Total number of tourist arrivals to the study area (million; [33]).

Years	Fethiye (F)	Muğla (M)	Turkey (T)	F/M (%)	M/T (%)	F/T (%)
2015	1.4	5.5	67.9	26.3	8.1	2.1
2016	0.9	4.6	59.4	19.9	7.8	1.6
2017	0.3	3.1	61.9	8.3	5.0	0.4
2018	0.4	3.9	71.9	9.5	5.5	0.5
2019	0.4	4.5	80.9	8.4	5.6	0.5
2020	0.3	2.3	41.9	11.7	5.5	0.6

2.2. LULC Retrieval

Information about LULC can serve many purposes such as following land development, loss and degradation resulting from human activities, their impacts on the environment, ecosystem services, land management, atmosphere and climate [2]. The concept of LULC focuses on the effects of the physical, chemical and cultural activities of humans on land [34]. LULC changes are determined using classification systems which identify and name the objects on the earth [35] and incorporate mapping and spatial data for object-based analyses. Object-based classification methods generally work with high accuracy using high-resolution satellite images [31] as in the present study. Satellite images are used to determine the spatial distribution or transformation of LULC classes representing different resolutions [36,37]. Remote sensing (RS) and geographic information systems (GIS) have long been used effectively for the determination of changes in LULC [31,38,39] with a combination of the required survey data and land information. Studies using satellite images to monitor LULC changes are varied in their aims and scopes like forested areas [40], water supply [41] and plant cover [42]. Different types of approaches are used to determine the changes in LULC and to identify the spatial differences in LULC patterns considering both temporal socio-economic and surface characteristics data [17,30,43].

Land surface and air temperatures (LST and AT) are affected by Earth's surface characteristics [43–45] and the size of changes in LST and AT is also affected by LULC changes especially in built-up areas [46–48] with a strong correlation with the normalised difference vegetation index (NDVI) and land cover changes caused by the urban built-up environment [49]. LST can be calculated using satellite images and the correlation between LST and changes in LULC is high, which gets higher with the increases in the amount of built-up surface and losses of natural lands [50].

Remote-sensing techniques were used in the present study for the assessment of the spatial and temporal LULC changes between 1995 and 2020 in Fethiye-Göcek SEPA as in other studies [30,31,51–53]. For this purpose, satellite images of Landsat-5 Thematic Mapper

(TM) for 6 July 1995; 28 July 2003 and Landsat-8 Operational Land Imager (OLI)/Thermal Infrared Sensor (TIRS) for 19 July 2020. These images were obtained from the United States Geological Survey (USGS). Mean accuracy values for each image are 0.96; 0.92 and 0.96, respectively, and each image was evaluated at 30 × 30 m spatial resolution (path/row: 188/33). Data were classified in the ERDAS Imagine 9.1. Great attention was paid to selecting each image in the same months and on cloudless days. First, a band joining process was performed on the supplied Landsat satellite images. After joining, the image bands were corrected radiometrically and geometrically (100 control points were used for geometric correction). The images were classified in an uncontrolled manner according to the ISODATA (Iterative Self-Organising Data Analysis) algorithm. Classification was made by assigning 100 classes to each of the images in 4-3-2 band combinations where the colour distribution is closer to the actual cover. WGS 84 coordinate system was used and geo-rectified to zone 35. Landscape diversity was categorised according to the CORINE index, which contains 44 classes and three LULC data levels, the first of which was employed in the study.

2.3. LST Retrieval

Because different land uses represent different heat absorption rates and emissivity, which result in LST fluctuations [54], parameters such as the percentage of built-up areas, vegetation, water bodies, agricultural and bare lands and rocky terrains are also considered to be the dominant land characteristics. Since the aim of the study is to determine the changes in the size of LULC in the study area, changes in the spatial distribution of LST were followed during the study period through Landsat 5-7-8 satellite imagery in the hottest summer months. Landsat TM/ETM+ images (band 6) and Landsat developed imaginary of 8 Thermal Infrared Sensors (OLI/TIRS) (two bands 10 and 11) and Radiative Transfer Equation (RTE) method were used to calculate LST. Images of each study year were computed and subjected to geometric corrections. The single channel algorithm and a combination of supervised image classification techniques were used to derive LST and for mapping the periodic changes in LULC. A mono-window algorithm was also used for the retrieval of LST from Landsat 5 TM band 6, Landsat 7 ETM+ band 6 and Landsat 8 OLI/TIR band 10-11. LST was computed using Equation (1) and the stages in the flowchart in Figure 2.

$$LST = \frac{TB}{1 + (ƛ x TB/þ) ln\varepsilon} \tag{1}$$

where TB is effective at satellite temperature in K, ƛ is the wavelength of emitted radiance (th = 11.5 μm), þ is 1.438 × 10^{-2} m K and ε is the wavelength efficiency [55,56].

The following equations were used at the stages given in Figure 2.

1. Conversion Digital Number (DN) to TOA Radiance

$$L\gamma = \left(\frac{LMAX\lambda - LMIN\lambda}{QCALMAX - QCALMIN}\right) \cdot (QCAL - QCALMIN) + LMIN\lambda$$

$$L\gamma = \left(\frac{15.303 - 1.238}{255 - 1}\right) \cdot (BAND6 - 1) + 1.238$$

2. Convert radiance into Brightness Temperature (BT) (ln Kelvin)

$$T = K2/ln\left(\frac{K1}{L\lambda} + 1\right)$$

$$T = 1260.56/ln\left(\frac{607.76}{Radiance\ value} + 1\right)$$

3. Convert Degree Kelvin into degree Celsius

$$C = T - 273.15$$

where:

T = Effective satellite temperature in Kelvin
K2 = Calibration constant 2 (1260.56 for Landsat 5 TM)
K1 = Calibration constant 1 (607.76 for Landsat 5 TM)
Lλ = Spectral radiance in (Watts/(m^2·sr·µm))
QCAL = Quantized calibrated pixel value in DN
LMAXλ = Spectral radiance scaled to QCALMAX in (Watts/(m^2·sr·µm))
LMINλ = Spectral radiance scaled to QCALMIN in (Watts/(m^2·sr·µm))
QCALMIN = Minimum quantized calibrated pixel value in DN
QCALMAX = Maximum quantized calibrated pixel value in DN

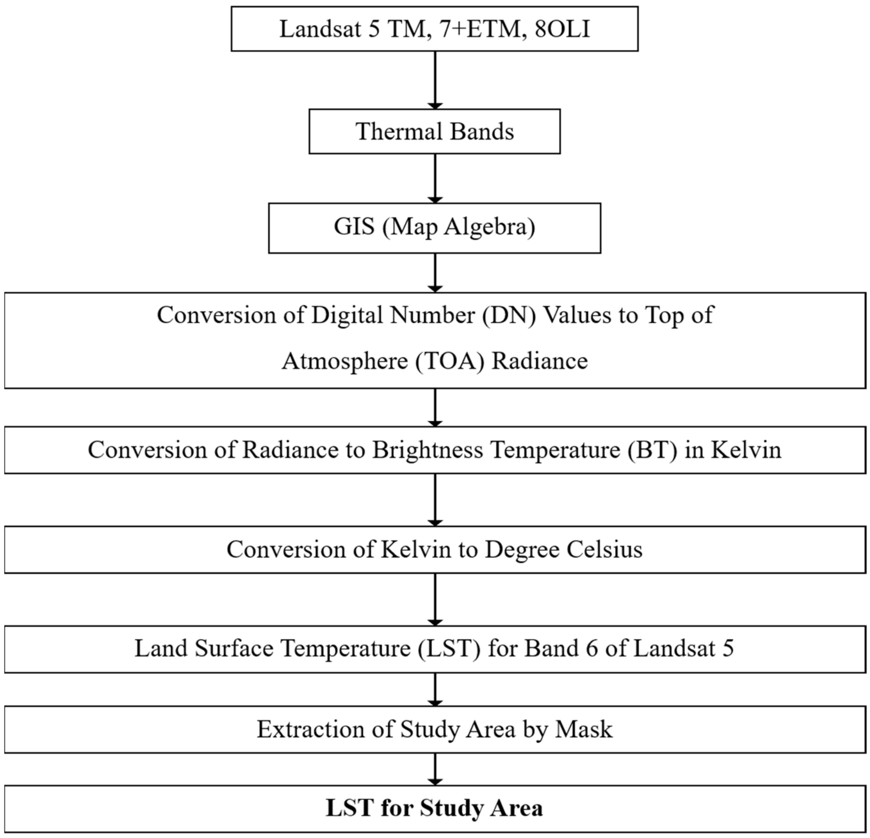

Figure 2. LST flowchart for ArcGIS.

2.4. NDVI Retrieval

NDVI is the representative of the vegetation covered surfaces [57] in the study. Index values show the temperature differences for the ecological characteristics of surfaces (e.g., green or brown surfaces). Equation (2) was used to determine NDVI as a ratio of measured reflectance in the red to near infrared (NIR) spectral bands.

$$\text{NDVI} = \frac{near\ IR\ band - red\ band}{near\ IR\ band + red\ band} \tag{2}$$

The index band changes from −1 to +1. The higher value indicates higher vegetation cover. Green vegetation has a higher reflectance value [58,59].

3. Results and Discussion

Three clustered maps were produced to classify LULC considering supervised maximum likelihood classification. Six LULC classes were identified in the CORINE legend; water surface, urban fabric, farmland, forest, shrubs and others (little or no vegetation like naked surfaces; [60,61]). The water surfaces as a class consist of sea, lake, river and wetlands and represent the largest surface area within the borders of Fethiye-Göcek SEPA. Both sea and land surfaces are included in the boundaries of the study area due to their protection status. The population of the Fethiye district in both its rural and urban area is 177,702 and the study area covers nearly 105,000 people with the population increase rate of nearly 3% a year [62]. It is interesting to find in the study that even though the area has been under protection for a long time due to the presence of sea turtles and endemic plant species, the total water surface area covered 34,561 ha in 1995, which decreased by approximately 331 ha in 2003 and 337 ha in 2020 (Table 3). This shows the loss (shrinkage) is not only on lands but also in the sea due to land reclamation (filling the sea and coastal areas to open lands for new functions), drying wetlands in spite of their legal protection status. Such areas are produced for urban development, constructing new buildings and facilities for touristic aims as the area is close to the city centre (Figure 3). As can be seen also in Table 3, the largest increase is experienced in urban fabrics with 4675 ha compared to 1995.

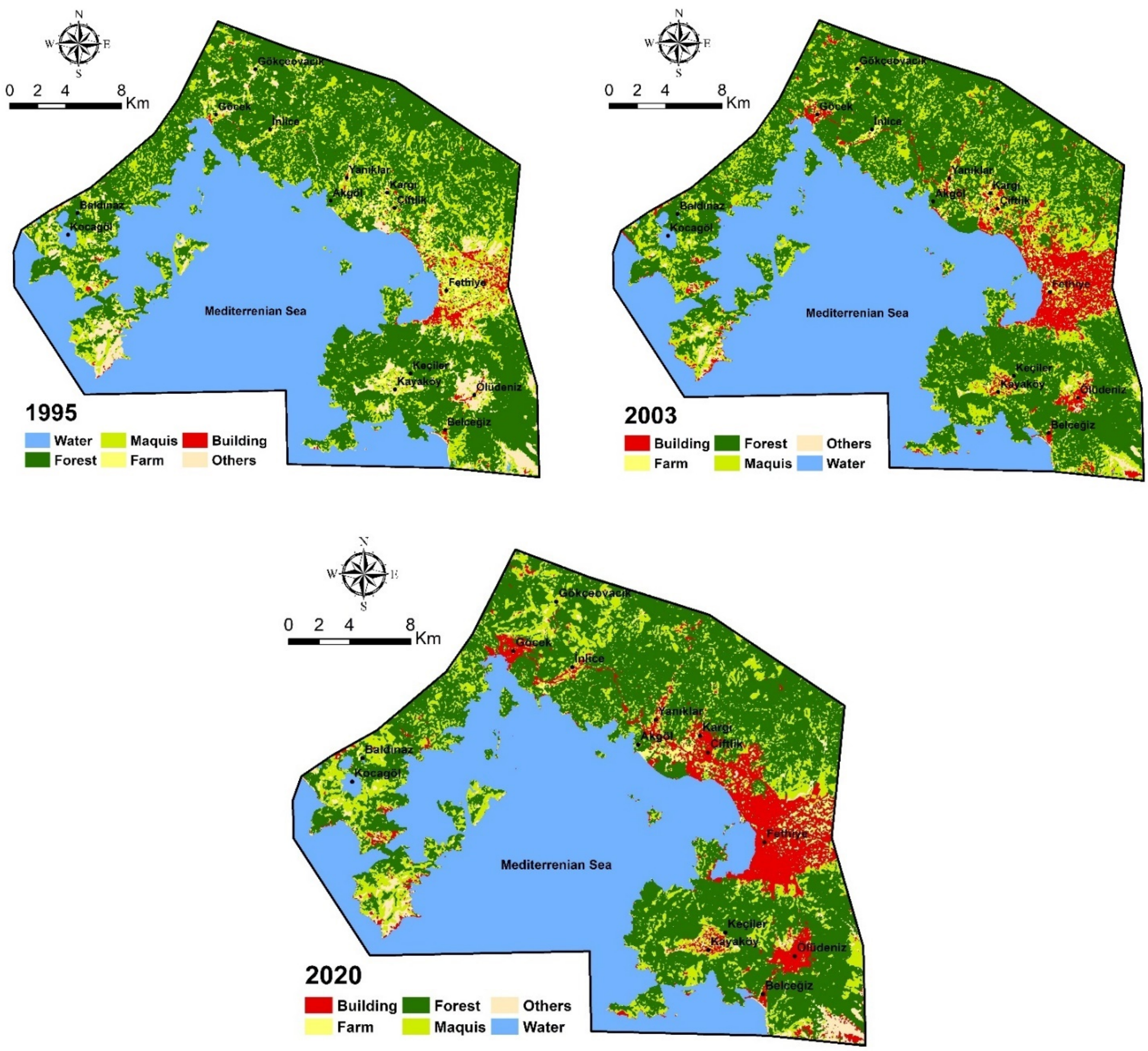

Figure 3. Comparing the spatial distribution of the changes in LULC between 1995, 2003 [63] and 2020.

Such changes in both land and sea surfaces are also monitored for the past and future [64] in order to detect the impacts of both human activities and climate change (sea levels rise). Land reclamation by filling the sea with debris is a really problematic situation for the future when considering climate hazards, however; many examples can be seen in the coastal parts of Turkey where land prices are high like Istanbul [65]. The size of forest cover in the study area was 27,895 ha at the beginning (1995), but decreased by 329 ha in 2003 and reached 27,181 ha in 2020. Among the causes of this decrease are forest fires and opening the land for agricultural activities. The total decrease in forest area reached 714 ha between 1995 and 2020. Forest area is composed mostly of red pine trees. The maquis (shrub) flora, which is mixed with red pine forests, consists of oak and olive trees. The maquis covered area also decreased by 1055 ha between 2003 and 2020 depending on large-scale forest fires. Monitoring the loss and damages of fires on forest areas is an important point in the Mediterranean region, where there is an increase in the frequency and periods of fires [66]. Another important point is the reforestation activities after fires without giving any functions on burnt areas in the study area [31].

In 1995, a majority of the area was covered by water surface and the water surface temperature was detected to vary between 18 and 20 °C. Land reclamation by filling the sea for developing urban use reduced the water surface area. In the existing and newly opened urban areas, the population reached up to 85,000 and the surface temperature was calculated to be 40 to 45 °C. As a result of these changes between 1995 and 2003, the transformation of water surfaces (decreasing by 337 ha) into structured urban surfaces also triggered the formation of urban heat islands (UHI). During this period, thermal properties of the surfaces also changed and surface temperatures increased greatly (as shown in other studies like [51,67–75]). From the surface image for 2020, the temperature change can be seen at the junction of the coastline with the sea up to 40 °C. Losses in agricultural lands are also reflected in temperature maps. Due to the transformation of agricultural lands into urban and structured areas in the study period, the temperature change is also higher in the LST map for the whole period (Table 3).

Table 3. LULC changes in 1995 and 2003 [63] and 2020 and between the study years.

LULC Types	Changes for the Years (ha)			Changes for the Periods (ha)			Trend
	1995	2003	2020	1995–2003	2003–2020	1995–2020	
Water (Sea, lake, river wetland)	34,561	34,230	34,224	331	6	337	Decrease
Forest (Coniferous, broad leaved)	27,895	27,566	27,181	329	385	714	Decrease
Maquis	12,289	12,982	11,927	−693	1055	362	Decrease
Farm (Planted, greenhouses)	1840	1511	930	329	581	910	Decrease
Building (Urban fabric)	**1159**	**4078**	**5834**	**−2919**	**−1756**	**−4675**	**Increase**
Others (Bare lands, coastal sands	3858	1235	1506	2623	−271	2352	Decrease

Surfaces representing agricultural lands cover cultivated–planted areas and greenhouses. Agricultural activities are carried out mostly in greenhouses in the study area. From 1995 to 2020, in total 910 ha agricultural land was lost to various uses, mainly construction/urbanisation since these areas are in close proximity to urban areas. Built-up urban areas converted from agricultural lands rapidly reached up to 2919 ha between 1995 and 2003 and 1756 ha between 2003 and 2020. Such changes in agricultural areas are seen in some other studies like [76,77], where similar reasons with the present study are proposed such as urbanisation, land price increases and industrial areas. With the increasing awareness among local people for the protection of lands, speed of the losses slowed down in recent years. A decrease is observed in the rate of transformation of agricultural and forestry areas into constructional areas. While there was a decrease of 2623 ha initially (1995–2003) in other areas consisting of open surface and coastal beaches depending on the urbanisation speed, a slight increase (271 ha) has been observed in recent years (Table 3). The rapid increase in the afforestation activities in the last decade has also lowered the rate of the transformation of other LULC into urban area.

LST computation results reflected the maximum temperatures on built-up and naked (without vegetation cover) surfaces (nearly 40 °C) and minimum on forested areas. LST maps also reveal that open surfaces, i.e., sand and bare rocks, reflect temperature values up to 40 °C and depending on the density of vegetation cover, temperatures range between 15 °C and 20 °C in maquis covered areas and red pine forests. Unfortunately, temperatures observed in urban surfaces reached up to 45 °C. In addition, high temperature values are also seen in the forests in the northern part of the study area due to enlarging village settlements in the forests where structural materials are used densely even if they appear as small points (Figure 4).

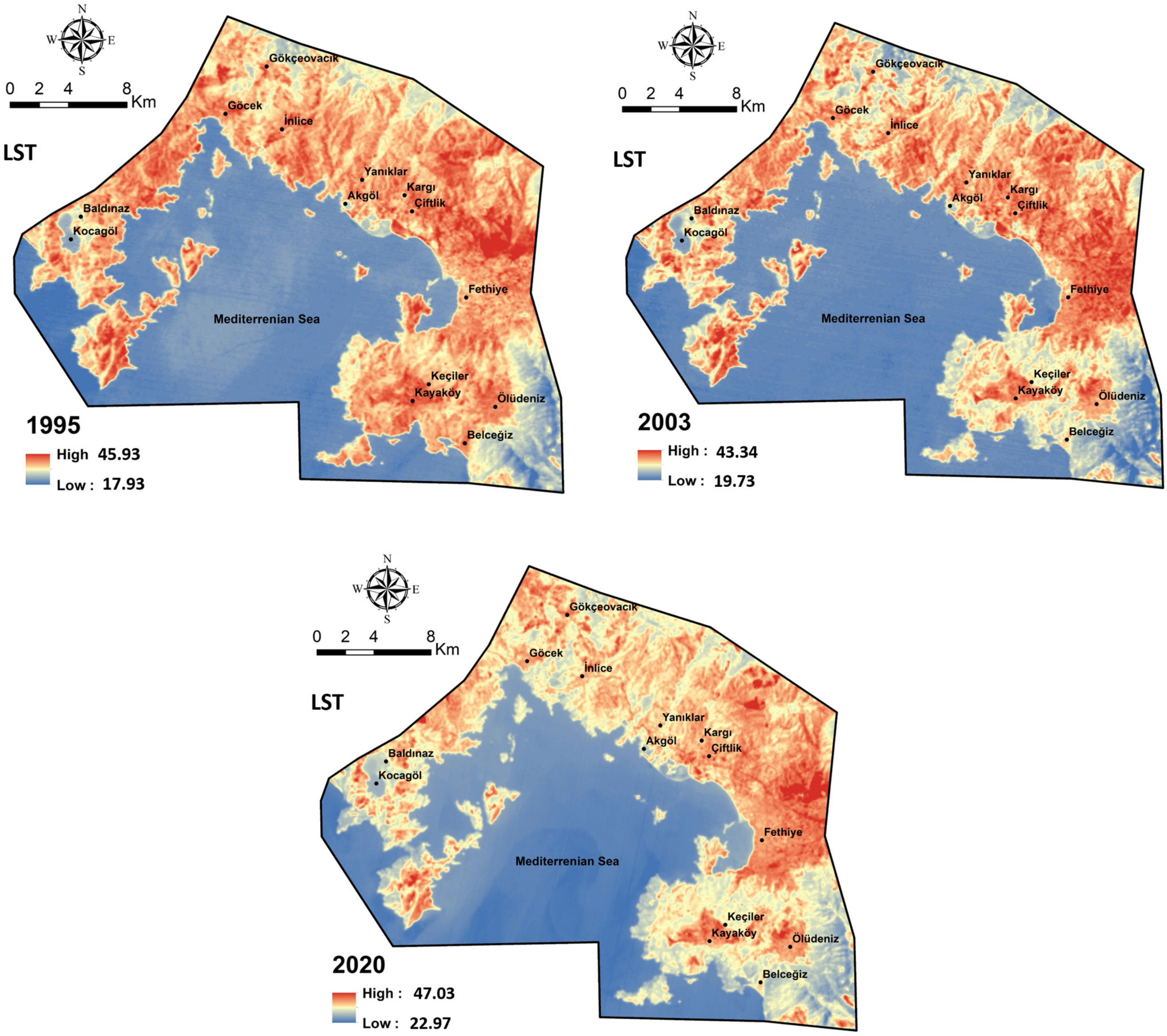

Figure 4. Spatial distribution of LST in the study years.

Relationship between the changes in LULC (ha) and LST (°C) was determined using a simple linear regression model. The correlation was found to be significant at 0.05 level ($p < 0.05$; Figure 5).

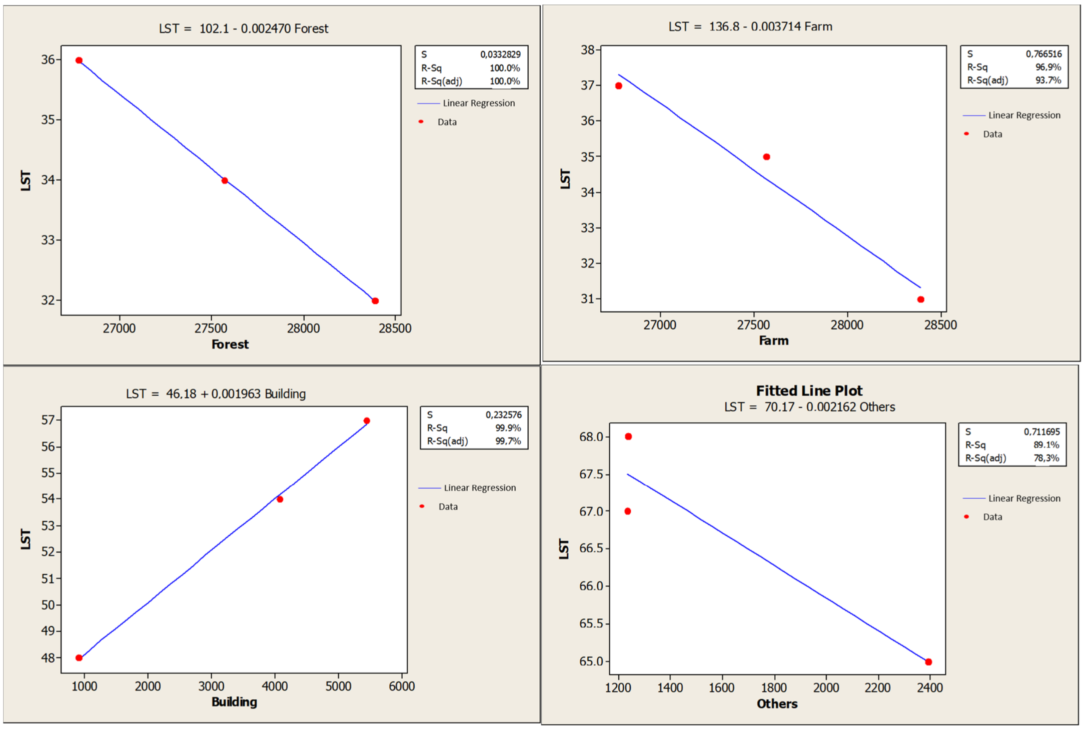

Figure 5. Linear regression model for LST and LULC.

According to statistical evaluation, both forest and agricultural lands show a negative correlation with LST while built-up urban lands have positive correlation. The relationship between the changes in LULC and LST reflected that the forested areas (coniferous) and water surfaces (sea) correspond to the minimum, deciduous forests and agricultural lands moderate, and rural and urban settlements, naked soil surfaces and burned forest areas maximum LST, which was observed to vary depending on the evaluated parameters like water surface and vegetation cover. It was found that a 10-percent rise in vegetation density led to a decrease in LST by approximately 1.3 °C. LST is about 14 °C in forest and 45 °C in urban structured surfaces (Figure 6). NDVI indices were taken as <0.2 for computational evaluation. The highest NDVI values were found over the dense vegetation areas while the lowest NDVI was observed over urban built-up areas, barren lands and water bodies (Figure 6).

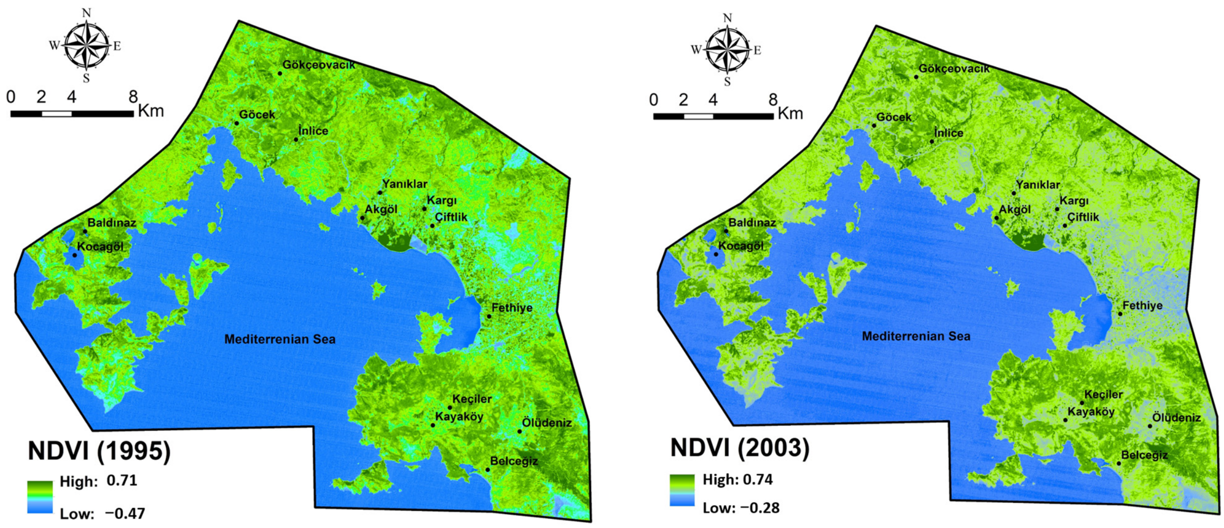

Figure 6. *Cont.*

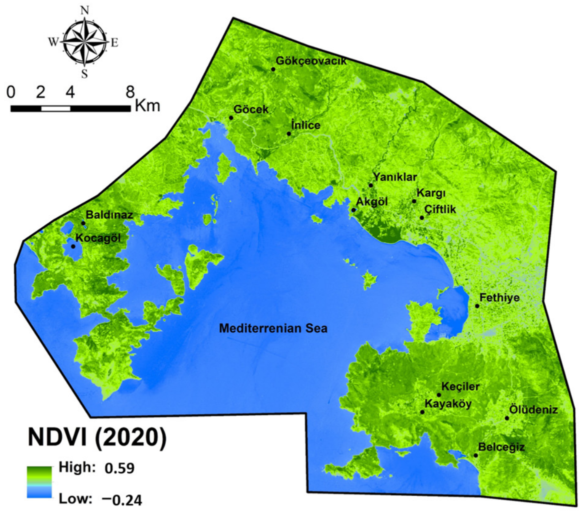

Figure 6. Spatial distribution of NDVI in the study years.

NDVI and LST are affected by several physical and climatic factors like vegetation, solar radiation and surface air temperature, rainfall and others [51,75,78–81], and a strong negative relationship is present between them as expected in all study years. In built-up areas, NDVI causes a very significant cooling effect in the study area (as it does in other studies like [82]; Figure 7).

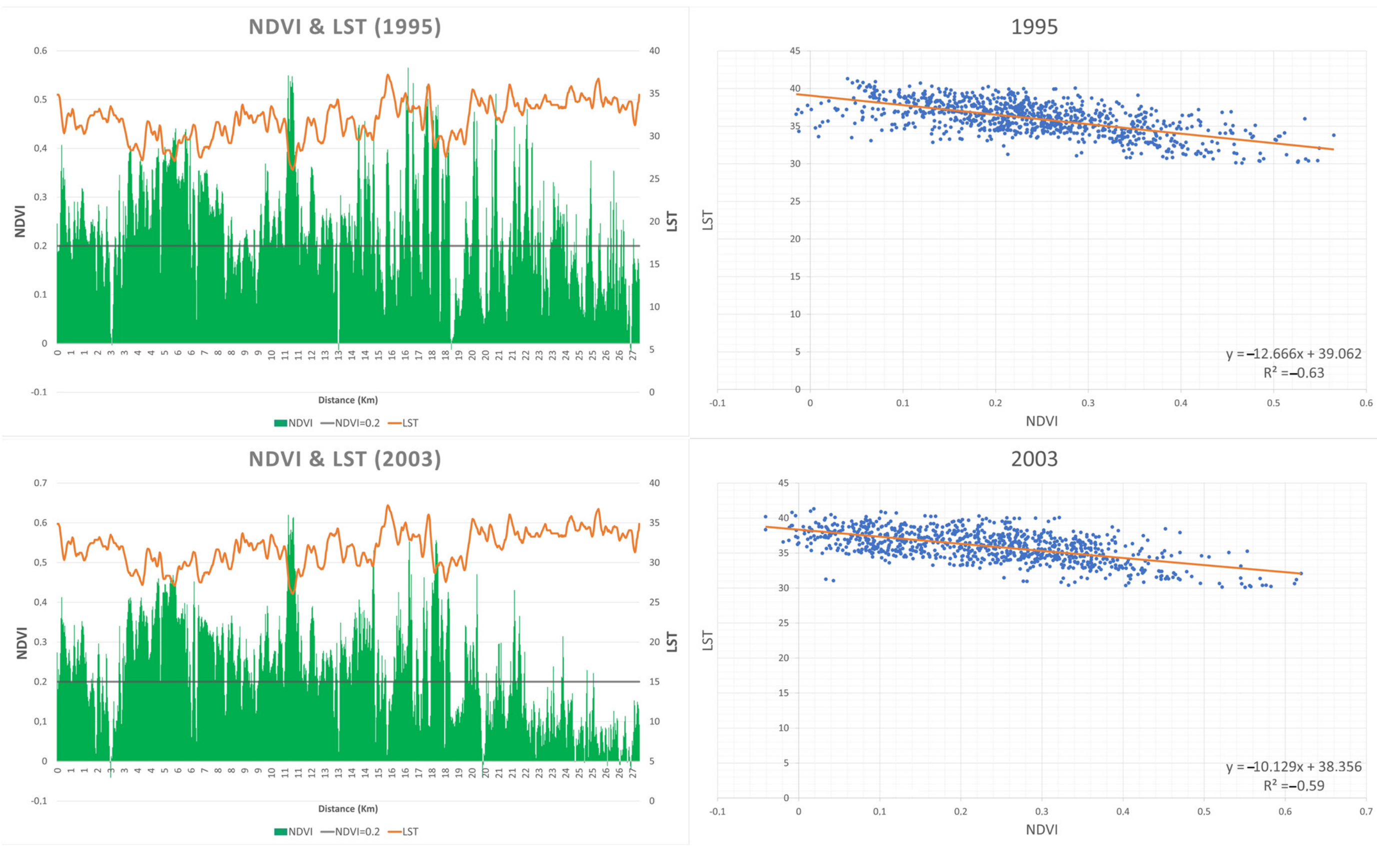

Figure 7. *Cont.*

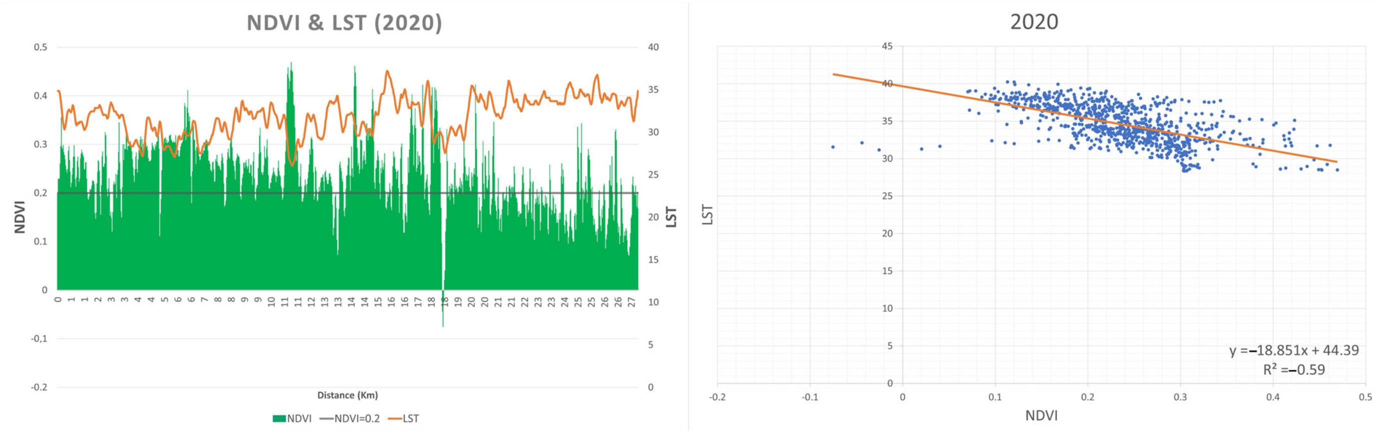

Figure 7. The relationship between NDVI and LST in the study area and study period.

A negative relationship/correlation between vegetated land and LST also continues in all years as detected in previous studies [74,83,84]. The regression coefficient was obtained as −0.63 for 1995 and −0.59 for both 2003 and 2020. The reason for the smaller regression is the loss of forest, maquis and farm lands.

Turkey's Mediterranean region is exposed to rapid tourism development and related human activities, especially urbanisation depending on tourism development. Therefore, various rates of LULC changes have been experienced as determined in previous studies. In such a study [29], land use changes in South Antalya were detected over the past 30 years with their impacts on agricultural lands and natural forests (816 and 457, respectively) for constructing tourism facilities like hotels, service buildings and settlements. Another study [30] carried out for the adjacent two peninsulas to the study area, Datça and Bozburun, where tourism activities have developed more recently than the study area and Bodrum used a similar methodology and period (1997–2018). The mentioned study showed that construction, road opening and tourism activities caused the changes in land cover between 1997 and 2018 in coastal and forest areas as in the present study. In a similar study [31] conducted over the same province with the study area but a different world-famous tourism district, Bodrum, including nearly the same period (1990–2021) and using a similar methodology, land cover change was detected due to the development of tourism activities. Main land cover change types are urban fabrics and burnt forest areas which appeared frequently after marine and coastal tourism developed while forests and semi-natural areas decreased.

4. Conclusions

It is interesting to see that the study area is a specially protected area, however lands are lost for economic activities in the area. The study was conducted using high-resolution surface data for spatial analysis. According to the results of the analysis over a 25-year period, when tourism activities and dependent land transformation showed a constantly increasing trend, mainly the water surface (i.e., sea) has been converted into a structured surface by filling the sea which is among the most hazardous activities due to the climate change-related sea level increase. Another LULC change is observed in the same period from forestlands to structured or urban lands due to touristic infrastructure, facilities and urban expansion/sprawl in order to open areas for housing human populations which has increased due to tourism development. Severity of LULC changes is the highest at the coastal zone even though the protection status of the area also includes the water surface. Even the interior part of the area (deep forest in the north) was exposed to this transformation from forest to structured surface due to the enlargement of rural settlements and use of unsuitable construction materials in the protected area. During the study period, the surface area of urban settlement increased continually while that of forest and farmland decreased especially in the plain areas in the coastal zone. The booming of tourism activities caused serious unplanned developments, changed the LULC in the area by degrading landscape characteristics and forest/maquis cover and coastal lines. Unplanned structural developments driven by tourism and its subsectors has been causing losses in priceless natural and cultural heritages in the area. These losses are expected to increase depending on the impact of climate change. In such a case, the area will also lose its advantage and competitiveness as a world-famous tourism destination even though there is an increasing local awareness about sustainable and responsible tourism development.

Present conditions of the study area were determined to negatively impact the liveability conditions of both dwellers and tourists due to extremely high surface temperatures in the settlements by causing UHI effects. Urban open green spaces and water surfaces play an active role in reducing urban temperatures and presenting more liveable environments to people. Therefore, urban forests, green roofs and vertical gardens and water surfaces must be created or protected to supply an optimum cooling effect and bioclimatic comfort.

The results of the present study are expected to contribute to decision makers and tourism planners to perceive the relationship between the changes in LULC, LST and NDVI. The study area is under the legal protection status and some development plans were prepared and implemented by the responsible authorities with various aims. However, there are always discrepancies or conflicts between the decisions of plans from different authorities. In order to develop sustainable tourism together with sustainable LULC in the future, an unchangeable, participatory and adopted plan should be prepared considering the impacts of climate change and this plan should be implemented by obeying its decisions strictly. It is also thought that the results and the method used in the study can be preferred to monitor the future LULC changes periodically.

Author Contributions: Conceptualization, I.C. and Z.R.A.; Methodology, I.C. and Z.R.A.; Original draft preparation, I.C., Z.R.A. and S.T.; Writing, I.C., Z.R.A. and S.T.; Data curation, Z.R.A.; Supervision, S.T.; Reviewing and Editing, S.T. All authors have read and agreed to the published version of the manuscript.

Funding: This research received no external funding.

Institutional Review Board Statement: Not applicable.

Informed Consent Statement: Not applicable, the study did not use any human or animal subjects.

Data Availability Statement: The authors declare that the data supporting the findings of this study are available within the paper and Turkish State Meteorology Services.

Conflicts of Interest: The authors declare no conflict of interest.

References

1. Baede, A.P.M.; Ahlonsou, E.; Ding, Y.; Schimel, D.; Bolin, B.; Pollonais, S.; IPCC. The Climate System: An Overview Co-Ordinating 2018/03/TAR-01. 2018. Available online: https://www.ipcc.ch/site/assets/uploads/2018/03/TAR-01.pdf (accessed on 16 January 2024).
2. Nedd, R.; Light, K.; Owens, M.; James, N.; Johnson, E.; Anandhi, A.A. Synthesis of Land Use/Land Cover Studies: Definitions, Classification Systems, Meta-Studies, Challenges and Knowledge Gaps on a Global Landscape. *Land* **2021**, *10*, 994. [CrossRef]
3. IPCC. *Climate Change 1994: Radiative Forcing of Climate Change and an Evaluation of the IPCC IS92 Emission Scenarios*; Houghton, J.T., Meira Filho, L.G., Bruce, J., Lee, H., Callander, B.A., Haites, E., Harris, N., Maskell, K., Eds.; Cambridge University Press: Cambridge, UK; New York, NY, USA, 1994; 339p.
4. Li, W.; Bai, Y.; Chen, Q.; Hee, K.; Ji, X. Discrepant impact of land use land cover on urban heat island: A case study of Shangai, China. *Ecol. İndic.* **2014**, *47*, 171–178. [CrossRef]
5. Li, X.; Zhou, W.; Ouyang, Z.; Xu, W.; Zheng, H. Spatial pattern of green space affects land surface temperature: Evidence from the heavily urbanized Beijing metropolitan area China. *Landsc. Ecol.* **2012**, *27*, 887–898. [CrossRef]
6. Alpagun, H.; Doygun, H. Post-classification comparison of land cover using multitemporal Landsat and ASTER imagery: The case of Kahramanmaraş, Turkey. *Environ. Monit. Assess.* **2009**, *151*, 327–336.
7. Azadi, H.; Ho, P.; Hasfiati, L. Agricultural land conversion drivers: Acomparision between less developed, developing and developed countries. *Land Degrad. Dev.* **2010**, *10*, 1002–1037. [CrossRef]
8. Cinar, I. Assessing the correlation between land cover conversion and temporal climate change—A pilot study in coastal Mediterranean city, Fethiye Turkey. *Atmosphere* **2015**, *6*, 1102–1118. [CrossRef]

9. Hong, N.B.; Yabe, M. Improvement in irrigation water use efficiency: A strategy for climate change adaptation and sustainable development of Vietnamese tea production. *Environ. Dev. Sustain.* **2017**, *19*, 1247–1263. [CrossRef]
10. Tan, R.; Beckmann, V.; van den Berg, L.; Qu, F. Governing Farmland conversion: Comparing China with Netherland and Germany. *Land Use Policy* **2009**, *26*, 961–974. [CrossRef]
11. Wang, J.; Liu, Y. Tourism-Led Land-Use Changes and their Environmental Effects in the Southern Coastal Region of Hainan Island, China. *J. Coast. Res.* **2013**, *29*, 1118–1125. [CrossRef]
12. Lin, G.C.S.; Ho, S.P.S. China's land resources and land-use change: Insights from the 1996 land survey. *Land Use Policy* **2003**, *20*, 87–107. [CrossRef]
13. Lin, G.C.S.; Ho, S.P.S. The state, land system, and land development processes in contemporary China. *Ann. Assoc. Am. Geogr.* **2005**, *95*, 411–436. [CrossRef]
14. Lin, W.; Yu, T.; Chang, X.; Wu, W.; Zhang, Y. Calculating cooling extents of green parks using remote sensing. *Landsc. Urban Plan.* **2015**, *134*, 66–75. [CrossRef]
15. Liu, J.Y.; Zhang, Z.X.; Xu, X.L.; Kuang, W.H.; Zhou, W.C.; Zhang, S.W.; Li, R.D.; Yan, C.Z.; Yu, D.S.; Wu, S.X.; et al. Spatial patterns and driving forces of land use change in China during the early 21st century. *J. Geogr. Sci.* **2010**, *20*, 483–494. [CrossRef]
16. Xu, W. The changing dynamics of land-use change in rural China: A case study of Yuhang, Zhejiang Province. *Environ. Plan. A* **2004**, *36*, 1595–1615. [CrossRef]
17. Liu, Y.S.; Wang, L.J.; Long, H.L. Spatio-temporal analysis of land-use conversion in the eastern coastal China during 1996–2005. *J. Geogr. Sci.* **2008**, *18*, 274–282. [CrossRef]
18. Long, H.; Liu, Y.; Wu, X.; Dong, G. Spatio-temporal dynamic patterns of farmland and rural settlements in Su–Xi–Chang region: Implications for building a new countryside in coastal China. *Land Use Policy* **2009**, *26*, 322–333. [CrossRef]
19. Wu, D.W.; Zhang, X.L.; Mao, H.Y.; Wu, H. Socio-economic driving forces of land-use change in Fuzhou, the southeastern coastal area of China. In Proceedings of the 2008 International Workshop on Earth Observation and Remote Sensing Applications, Beijing, China, 30 June–2 July 2008; pp. 261–271.
20. World Data. 2023. Available online: https://www.worlddata.info/asia/turkey/tourism.php (accessed on 4 February 2024).
21. UNWTO. International Tourism Highlights 2020 Edition. 2020. Available online: https://www.e-unwto.org/doi/epdf/10.18111/9789284422456 (accessed on 4 February 2024).
22. Becken, S.; Scott, D. (Eds.) Tourism Panel on Climate Change. Tourism and Climate Change Stocktake. 2023. Available online: https://tpcc.info/ (accessed on 4 February 2024).
23. Gossling, S. The consequences of tourism for sustainable water use on a tropical island: Zanzibar, Tanzania. *J. Environ. Manag.* **2001**, *61*, 179–191. [CrossRef] [PubMed]
24. Rico-Amoros, A.M.; Olcina-Cantos, J.; Sauri, D. Tourist land use patterns and water demand: Evidence from the Western Mediterranean. *Land Use Policy* **2009**, *26*, 493–501. [CrossRef]
25. Matei, N.A.; García-León, D.; Dosio, A.; Batista e Silva, F.; Ribeiro Barranco, R.; Císcar Martínez, J.C. *Regional Impact of Climate Change on European Tourism Demand*; Publications Office of the European Union: Luxembourg, 2023.
26. Gossling, S. Global environmental consequences of tourism. *Glob. Environ. Change—Hum. Policy Dimens.* **2002**, *12*, 283–302. [CrossRef]
27. Esbah, H.; Kara, B.; Deniz, B.; Kesgin, B. Changing land cover characteristics of a developing coastal town: A case study of Didim, Turkey. *J. Coast. Res.* **2010**, *26*, 274–282. [CrossRef]
28. Kuvan, Y. The use of forests for the purpose of tourism: The case of Belek Tourism Center in Turkey. *J. Environ. Manag.* **2005**, *75*, 263–274. [CrossRef]
29. Atik, M.; Altan, T.; Artar, M. Land Use Changes in Relation to Coastal Tourism Developments in Turkish Mediterranean. *Pol. J. Environ. Stud.* **2010**, *19*, 21–33. Available online: http://www.pjoes.com/pdf-88352-22210?filename=Land%20Use%20Changes%20in.pdf (accessed on 4 February 2024).
30. İkiel, C.; Ustaoğlu, B.; Dutucu, A.A.; Kılıç, D.E. Determination of land cover change in Datça and Bozburun Peninsula in Turkey (1997–2018). In Proceedings of the 2019 8th International Conference on Agro-Geoinformatics (Agro-Geoinformatics), Istanbul, Turkey, 16–19 July 2019.
31. Ustaoğlu, B. Land cover change analysis between 1990 and 2021 using Landsat images and object-based classification: A case study in Bodrum peninsula, Aegean Region, Turkey. *Ege Coğrafya Derg.* **2022**, *31*, 101–119. [CrossRef]
32. MGM. Mean Climate Parameters. 2023. Available online: https://www.mgm.gov.tr/veridegerlendirme/il-ve-ilceler-istatistik.aspx?k=A&m=MUGLA (accessed on 21 January 2024).
33. Turkish Ministry of Culture and Tourism. Accommodation Statistics Provided by Turkish Ministry of Culture and Tourism. 2023. Available online: https://yigm.ktb.gov.tr/TR-201120/konaklama-istatistikleri.html (accessed on 4 February 2024).
34. Sreedhar, Y.; Nagaraju, A.; Murali Krishna, G. An Appraisal of Land Use/Land Cover Change Scenario of Tummalapalle, Cuddapah Region, India—A Remote Sensing and GIS Perspective. *Adv. Remote Sens.* **2016**, *5*, 232–245. [CrossRef]
35. Duhamel, C. Land Use and Land Cover, Including Their Classification. *Encyclopedia Life Support Syst.* **2012**, *1*, 9. Available online: https://www.eolss.net/Sample-Chapters/C12/E1-05-01-01.pdf (accessed on 4 February 2024).
36. Mishra, P.K.; Rai, A.; Rai, S.C. Land use and land cover change detection using Geospatial Techniques in Sikkim Himalaya, India. *Egypt. J. Remote Sens. Space Sci.* **2020**, *23*, 133–143. [CrossRef]

37. Sertel, E.; Musaoglu, N.; Alp, G.; Algan, Y.I.; Kaya, Ş.; Yüksel, B.; Yılmaz, A. 1:25.000 ölçekli ulusal arazi örtüsü/kullanımı sınıflandırma sistemi ile HGK TOPOVT veritabanının karşılaştırılması. *Harit. Derg.* **2018**, *160*, 34–46.
38. Fazal, S. Urban expansion and loss of agricultural land—A GIS based study of Saharanpur City, India. *Environ. Urban.* **2000**, *12*, 133–149. [CrossRef]
39. Lambin, E.F. Modelling and monitoring land-cover change processes in tropical regions. *Prog. Phys. Geogr.* **1997**, *21*, 375–393. [CrossRef]
40. Yavaşlı, D.D.; Masek, J.G.; Franks, S. Muğla İlinde 2000–2010 Yılları Arasındaki Orman Bozunum ve Geri Kazanımının Landsat Görüntüleri İle İzlenmesi. *Ege Coğrafya Derg.* **2013**, *22*, 91–106. Available online: https://dergipark.org.tr/en/pub/ecd/issue/4866/66878 (accessed on 21 January 2024).
41. Cüceloğlu, G.; Şeker, D.Z.; Tanık, A.; Öztürk, İ. SWAT Modeli Kullanılarak İki Farklı Arazi Kullanım Veri Kümesinin Hidrolojik Simülasyonlar Üzerindeki Etkilerinin İncelenmesi. *Uluslararası Çevre Jeoinformatik Derg.* **2021**, *8*, 172–185. [CrossRef]
42. İkiel, C.; Koç, D. Analysis of The Changes in Vegetation of The Sapanca Lake Basin (in Turkey) Using Multitemporal Satallite Data. *Int. J. Hum. Sci.* **2015**, *12*, 1095–1116.
43. Ren, J.; Yang, J.; Wu, F.; Sun, W.; Xiao, X.; Xia, J.C. Regional thermal environment changes: Integration of satellite data and land use/land cover. *iScience* **2023**, *26*, 105820. [CrossRef]
44. Paramanik, S.; Punia, M. Assessment of green space cooling effects in dense urban landscape: A case study of Delhi, India. *Mod. Earth. Syst. Environ.* **2018**, *5*, 867–884. [CrossRef]
45. Yin, C.; Yuan, M.; Lu, Y.; Huang, Y.; Liu, Y. Effect of urban form on the urban heat island effect based on spatial regression model. *Sci. Total Environ.* **2018**, *634*, 696–704. [CrossRef] [PubMed]
46. Chen, A.; Yao, L.; Sun, R.; Chen, L. How many metrics are required to identify the effects of the landscape pattern on land surface temperature. *Ecol. Indic.* **2014**, *45*, 424–433. [CrossRef]
47. Chen, Y.; Yang, J.; Yu, W.; Ren, J.; Xiao, X.; Xia, J.C. Relationship between urban spatial form and seasonal land surface temperature under different grid scales. *Sustain. Cities Soc.* **2023**, *89*, 104374. [CrossRef]
48. Cinar, İ.; Cicek, İ.; Ardahanlioglu, Z.R.; Karakus, N. Thermal comfort assessment of the urban Mediterranean climate, South-west Anatolia, Turkey. *Int. J. Adv. Sci. Eng. Technol.* **2013**, *4*, 3.
49. Shi, H.; Chen, J. Charesteristic of climate change and its relationship with land use/cover change in Yunna Province, China. *Int. J. Clim.* **2018**, *38*, 2520–2537. [CrossRef]
50. Zhang, J.L.; Pham, T.-T.-H.; Kalacska, M.; Turner, S. Using Landsat Thematic Mapper records to map land cover change and the impacts of reforestation programmes in the borderlands of southeast Yunnan, China: 1990–2010. *Int. J. Appl. Earth Obs. Geoinf.* **2011**, *31*, 25–36. [CrossRef]
51. Dadashpoor, H.; Khaleghinia, A.; Shabrang, A. Explaining the role of land use changes on land surface temperature in an arid and semi-arid metropolitan area with multi-scale spatial regression analysis. *Environ. Monit. Assess.* **2024**, *196*, 124. [CrossRef] [PubMed]
52. Dewan, A.M.; Yamaguchi, Y. Land use and land cover change in Greater Dhaka, Bangladesh: Using remote sensing to promote sustainable urbanization. *Appl. Geogr.* **2009**, *29*, 390–401. [CrossRef]
53. Ma, Y.; Wu, H.P.; Wang, L.Z.; Huang, B.M.; Ranjan, R.; Zomaya, A.; Jie, W. Remote sensing big data computing: Challenges and opportunities. *Future Gener. Comp. Syst.* **2015**, *51*, 47–60. [CrossRef]
54. Zhao, C.; Jensen, J.; Weng, Q.; Weaver, R. A geographically weighted regression analysis of the underlying factors related to the surface Urban Heat Island Phenomenon. *Remote Sens.* **2018**, *10*, 1428. [CrossRef]
55. Ekwe, M.C.; Adamu, F.; Gana, J.; Nwafor, G.C.; Usman, R.; Nom, J.; Onu, D.O.; Adedejı, O.I.; Halilu, S.A.; Aderoju, O.M. The effect of green spaces on the urban thermal enviroment during a hot-dry season: A case stufy of Port Harcourt, Nigeria. *Environ. Dev. Sustain.* **2020**, *23*, 10056–10079. [CrossRef]
56. Qin, Z.-H.; Karnieli, A.; Berliner, P. A mono-window algorithm for retrieving land surface temperature from Landsat TM data and its application to the Israel-Egypt border region. *Int. J. Remote Sens.* **2001**, *22*, 3719–3746. [CrossRef]
57. Weng, Q.; Lu, D.; Schubring, J. Estimation of land surface temperature-vegetation abundance relationship for urban heat island studies. *Remote Sens. Environ.* **2004**, *89*, 467–483. [CrossRef]
58. Oguz, H. LST calculator: A program for retrieving land surface temperature from Landsat TM/ETM+ imagery. *Environ. Eng. Manag. J.* **2013**, *12*, 549–555. [CrossRef]
59. Oguz, H.; Doygun, N.; Kısakürek, S.; Özcalık, M. Calculating surface temperature of Izmir, Turkey. *J. Archit. Eng. Fine Arts* **2019**, *1*, 36–46.
60. Hardwick, S.R.; Ralf, T.; Marion, P.; Eadgar, T.; Reuben, N.; Ewers, R.M. The relationship between the leaf area index and microclimate in tropical forest and oil plant plantation: Forest disturbance drives changes in microclimate. *Agric. For. Meteorol.* **2015**, *201*, 187–195. [CrossRef]
61. Wang, R.; Hou, H.; Derdoni, A. Spatiotemporal Analysis of Land Use/Cover Patterns and Their Relationship with Land Surface Temperature in Nanjing, China. *Remote Sens.* **2020**, *12*, 440. [CrossRef]
62. Turkish Statistics Institution. Population of Province/District Centers and Towns/Villages and Annual Population Growth Rate by Province, 2021, 2022. 2023. Available online: https://data.tuik.gov.tr/Bulten/Index?p=49685 (accessed on 4 February 2024).

63. Ardahanlioglu, Z.R. The Evaluation of Changes in the Usage of Area Within Ecological Planning in Fethiye Göcek Special Protection Area. Ph.D. Thesis, Ataturk University, Graduate School of Natural and Applied Sciences, Department of Landscape Architecture, Yakutiye, Türkiye, 2014; 269p.
64. Lopes, N.D.R.; Li, T.; Zhang, P.; Matomela, N.; Ikhumhen, H.O.; Sá, R.M. Predicting future coastal land use/cover change and associated sea-level impact on habitat quality in the Northwestern Coastline of Guinea-Bissau. *J. Environ. Manag.* **2023**, *327*, 116804. [CrossRef]
65. Şimşek, Ç.K.; Arabacı, D. Simulation of the climatic changes around the coastal land reclamation areas using artificial neural networks. *Urban Clim.* **2021**, *38*, 100914. [CrossRef]
66. Çolak, E.; Sunar, F. Evaluation of forest fire risk in the Mediterranean Turkish forests: A case study of Menderes region, Izmir. *Int. J. Disaster Risk Reduct.* **2020**, *45*, 101479. [CrossRef]
67. Feizizadeh, B.; Blaschke, T. Examining urban heat island relations to land use and air pollution: Multiple end member spectral mixture analysis for thermal remote sensing. *IEEE J. Sel. Top. Appl. Earth Obs. Remote Sens.* **2013**, *6*, 1749–1756. [CrossRef]
68. Sarrat, C.; Lemonsu, A.; Masson, V.; Guedalia, D. Impact of urban heat island on regional atmospheric pollution. *Atmos. Environ.* **2006**, *40*, 1743–1758. [CrossRef]
69. Silva, J.S.; da Silva, R.M.; Santos, C.A.G. Spatiotemporal impact of land use/land cover changes on urban heat islands: A case study of Paço do Lumiar, Brazil. *Build. Environ.* **2018**, *136*, 279–292. [CrossRef]
70. Simwanda, M.; Ranagalage, M.; Estoque, R.C.; Murayama, Y. Spatial analysis of surface urban heat Islands in four rapidly growing african cities. *Remote Sens.* **2019**, *11*, 1645. [CrossRef]
71. Singh, P.; Kikon, N.; Verma, P. Impact of land use change and urbanization on urban heat island in Lucknow city, Central India. A remote sensing -based estimate. *Sustain. Cities Soc.* **2017**, *32*, 100–114. [CrossRef]
72. Siqi, J.; Yuhong, W. Efects of land use and land cover pattern on urban temperature variations: A case study in Hong Kong. *Urban Clim.* **2020**, *34*, 100693. [CrossRef]
73. Solecki, W.D.; Rosenzweig, C.; Parshall, L.; Pope, G.; Clark, M.; Cox, J.; Wiencke, M. Mitigation of the heat island effect in urban New Jersey. *Glob. Environ. Chang. B Environ. Hazards* **2005**, *6*, 39–49. [CrossRef]
74. Tran, H.; Uchihama, D.; Ochi, S.; Yasuoka, Y. Assessment with satellite data of the urban heat island effects in Asian mega cities. *Int. J. Appl. Earth Obs. Geoinf.* **2006**, *8*, 34–48. [CrossRef]
75. Weng, Q. A remote sensing-GIS evaluation urban expansion and its impact on surface temperature in the Zhujian Delta, China. *Int. J. Remote Sens.* **2001**, *10*, 1999–2014.
76. Seyam, M.H.; Haque, R.; Rahman, M. Identifying the land use land cover (LULC) changes using remote sensing and GIS approach: A case study at Bhaluka in Mymensingh, Bangladesh. *Case Stud. Chem. Environ. Eng.* **2023**, *7*, 100293. [CrossRef]
77. Wang, H.; Feng, Q.; Ruan, X. Loss or gain: A spatial regression analysis of switching land conversion between agriculture and natural land. In *Ecosystems and Environment*; Elsevier: Amsterdam, The Netherlands, 2016; pp. 222–234.
78. Churkina, G.; Running, S.W. Contrasting climatic controls on the estimated productivity of global terrestrial biomas. *Ecosystems* **1998**, *1*, 206–215. [CrossRef]
79. Cohen, P.; Potchter, O.; Matzarakis, A. Daily and seasonal climatic conditions of green urban open spaces in the Mediterranean climate and their impacton human comfort. *Build. Environ.* **2012**, *51*, 285–295. [CrossRef]
80. Hidalgo-García, D.; Arco-Díaz, J. Modeling the Surface Urban Heat Island (SUHI) to study of its relationship with variations in the thermal feld and with the indices of land use in the metropolitan area of Granada (Spain). *Sustain. Cities Soc.* **2022**, *87*, 104166. [CrossRef]
81. Karnieli, A.; Agam, N.; Pinker, R.C.; Anderson, M.; Imhoff, M.; Gutman, G.G.; Panov, N.; Goldberg, A. Use of NDVI and Land Surface Temperature for Drought Assessment: Merits and Limitations. *J. Clim.* **2009**, *23*, 618–633. [CrossRef]
82. Abulibdeh, A. Analysis of urban heat island characteristics and mitigation strategies for eight arid and semi-arid gulf region cities. *Environ. Earth Sci.* **2021**, *80*, 259. [CrossRef]
83. Bokaie, M.; Zarkesh, M.K.; Aresteh, P.D.; Hasseini, A. Assessment of urban heat island based on the relationship between land surface temperature and land use/land cover in Tehran. *Sustain. Cities Soc.* **2016**, *23*, 94–104. [CrossRef]
84. Kaplan, G.; Avdan, U.; Avdan, Z.Y. *Urban Heat Island Analysis using Landsat 8 Satellite Data: A Case Study in Skopje, Macedonia*; Multidisiplinary Dijital Publishing Institute Proceedings: Basel, Switzerland, 2018; Volume 2, p. 58.